Eur. Phys. J. B **46**, 231–235 (2005)
DOI: 10.1140/epjb/e2005-00251-y

THE EUROPEAN PHYSICAL JOURNAL B

Percolation limited magnetic order in $Eu_{1-x}Ca_xB_6$

G.A. Wigger[1,a], E. Felder[1], M. Weller[1], S. Streule[1], H.R. Ott[1], A.D. Bianchi[2], and Z. Fisk[3]

[1] Laboratorium für Festkörperphysik, ETH-Hönggerberg, 8093 Zürich, Switzerland
[2] National High Magnetic Field Laboratory, Florida State University, Tallahassee, Florida 32306, USA
[3] Department of Physics, University of California - Davis, CA 95616, USA

Received 27 January 2005 / Received in final form 29 April 2005
Published online 11 August 2005 –

Abstract. We report the results of measurements of the low-temperature specific heat $C_p(T)$ and the ac susceptibility $\chi_{ac}(T)$ in low applied magnetic fields for a series of samples of $Eu_{1-x}Ca_xB_6$. The anomalies in $C_p(T)$, together with the results for $\chi_{ac}(T)$ and $M(H)$, confirm the onset of phase transitions to long range magnetic order for $x < 0.7$ and provide evidence that for $x \geq 0.7$, the Eu moments, which are captured in large magnetic clusters with magnetic moments of the order of 260 μ_B, adopt a spin-glass type ground state. The data set allows to establish the low-temperature [T,x] phase diagram of this alloy series.

PACS. 71.30.+h Metal-insulator transitions and other electronic transitions – 75.20.-g Diamagnetism, paramagnetism, and superparamagnetism

1 Introduction

The phenomenon of magnetic order in solids is most often based on periodic arrays of magnetic moments on regular lattice sites, here denoted as magnetic sites, of the crystal structure of the respective material. The necessary interaction between the moments, which more or less determines the transition temperature and the ordered-moment configuration, may be due to different causes, not of primary interest here. The present work is devoted to investigating the influence of the random removal of magnetic moments on the onset of magnetic order at low temperatures.

A prominent example of magnetic systems is the so called Heisenberg ferromagnet, where all magnetic sites are occupied by moments, which are mutually linked by some interaction. The probability of finding an unbroken path following these links on a random path across the sample is $P = 1$. This situation is altered, if a number of moments is randomly removed from the magnetic sites, breaking all links to the respective nearest neighbour moments. The parameter P may also be defined as the probability of the existence of an infinitely large cluster of adjacent moments in an infinitely large array of such moments. In a three-dimensional simple cubic structure, the concentration of moments, below which $P = 0$, is $c_{thres} \approx 0.31$, the so called site percolation limit [1,2]. For $c < c_{thres}$ it is predicted that the ground state of the solid is no longer characterized by long range magnetic order and other configurations of the moments are energetically more favourable.

The hexaboride compound EuB_6 may be regarded as a model system for studying this site percolation problem. It crystallizes with a simple cubic structure. The Eu ions, each carrying a magnetic moment of 7 μ_B due to the half filled $S = 7/2$ 4f electron shell [3], occupy the centers of cubes whose corners are decorated with B_6 octahedra. Ferromagnetic order sets in at approximately 15 K. The chemical composition may be changed by, e.g., replacing the rare-earth element Eu by the alkaline earth element Ca. Because both type of ions adopt a divalent configuration, the substitution is in first order expected to be isoelectronic and simply provoking a dilution of magnetic moments. Recently published results of electronic transport measurements and their interpretation based on theoretical modelling suggested the influence of site percolation on the magnetic and transport properties of $Eu_{1-x}Ca_xB_6$ [4].

In this work we investigated the x-dependence of the magnetic properties of $Eu_{1-x}Ca_xB_6$ with measurements of the specific heat, the magnetic susceptibility and field induced magnetization at low temperatures. The results indicate that long range magnetic order among the Eu moments ceases to be established, if x exceeds 0.7 or, in view of site percolation, the concentration of magnetic moments $c < c_{thres}$. Instead, the ground state seems to adopt a spin-glass type configuration of the remaining Eu moments.

[a] e-mail: gwigger@standford.edu

The samples were all in single-crystalline form and their high structural quality was confirmed by corresponding characterizations using X-ray and electron-microscopy techniques. For more details, the reader should consult references [4,8,14].

2 Results and discussion

2.1 Specific heat

We first concentrate on our study of the low-temperature specific heat. The investigated samples were single crystals in the form of platelets and the compositions were such that $x = 0.1$, 0.16, 0.37, 0.65 and 0.77, respectively. The specific heat $C_p(T)$ was measured in the temperature range between 0.34 and 22 K, employing the conventional relaxation method. The $C_p(T)$ data for a crystal of the binary compound with $x = 0$ was taken from the work presented in reference [5]. Since we are mainly interested in the magnetic part of $C_p(T)$, we attempted to separate the different contributions. The dominant non magnetic term is due to lattice excitations, C_{latt}. The contribution due to conduction electrons can safely be neglected because their concentration is only of the order of 10^{-3} per unit cell. Earlier successful analyses of specific-heat and resistivity data of hexaborides were based on the assumptions that i) the excitations of the Boron network are sufficiently well accounted for by a Debye-type spectrum with $\theta = 1160$ K in the case of LaB_6 [6] and that ii) the cation motions are well represented by Einstein-type oscillators. Thus the molar specific heat of the lattice is

$$C_p^{lattice}(T) = C_p^{Debye}(T) + C_p^{Einstein}(T) \quad . \qquad (1)$$

The calculations of the two terms is done by using the well known integral expressions [23]. For this particular series, the element specific Einstein temperatures are $\theta_{Eu} = 168$ K for Eu [8] and $\theta_{Ca} = 373$ K for Ca [4], respectively. The second term on the rhs of equation (1) is thus concentration dependent and a sum of the form

$$C_p^{Einstein}(T) = (1-x) \cdot C_p^{Eu}(T) + x \cdot C_p^{Ca}(T) \quad , \qquad (2)$$

where $C_p^{Eu}(T)$ and $C_p^{Ca}(T)$ denote the contributions from the Eu- and Ca ions, respectively. We assume that the Debye temperature does not vary across the series.

The magnetic part $C_{mag}(T)$ of the specific heat is now obtained by simply subtracting the calculated lattice specific heat from the measured data. The result is shown in Figure 1. Although shifted to lower temperatures, the two consecutive transitions, clearly seen and discussed in previous work for EuB [5,9–12], persist to Ca contents of at least 16%. Only one transition is observed for $x = 0.37$ and beyond, confirming earlier conclusions based on results of electronic transport measurements [13,14]. We note that from comparing the shapes of the specific-heat anomalies for $x = 0.65$ and $x = 0.77$ alone, the transition from a ferromagnetically ordered to a spin-glass type ground state cannot be inferred.

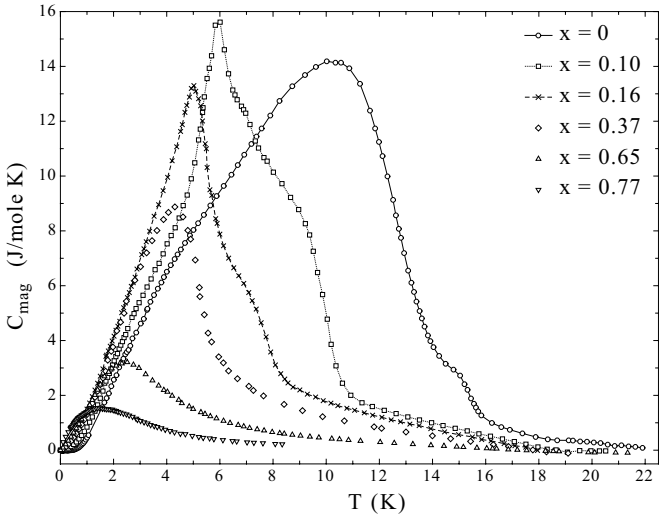

Fig. 1. Magnetic part of the specific heat for $x = 0$, 0.1, 0.16, 0.37, 0.65 and 0.77.

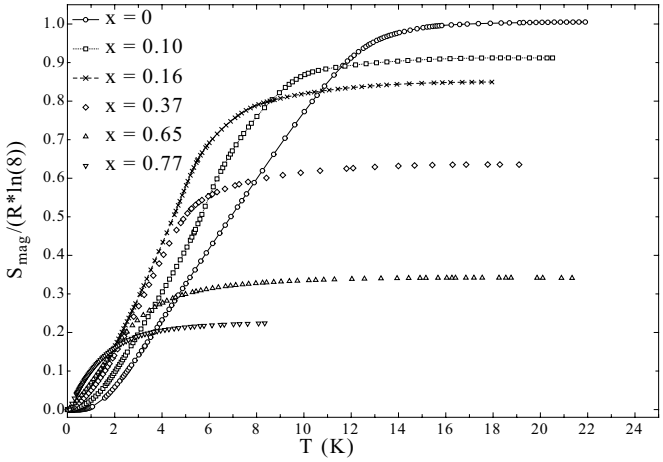

Fig. 2. Magnetic entropy for $x = 0$, 0.1, 0.16, 0.37, 0.65 and 0.77.

The magnetic entropy across these transitions is readily obtained from

$$S_{mag} = \int_0^T \frac{C_{mag}(T')}{T'} dT' \quad . \qquad (3)$$

As may be seen in Figure 2, the full molar magnetic entropy of the Eu^{2+} ions, which amounts to $(1-x)R\ln(2J+1)$ with $J = 7/2$, is recovered at approximately 20 K for all values of x covered in this study.

2.2 Magnetic susceptibility and magnetization

The magnetic phase diagram for $x < 0.7$ was established by Arrott-plot analyses in combination with specific-heat and susceptibility experiments [4]. In order to probe the magnetic properties of those alloys with $x > 0.7$ and hence for moment concentrations $c < c_{thres}$, we measured the ac magnetic susceptibility χ_{ac} of $Eu_{1-x}Ca_xB_6$ between 0.35

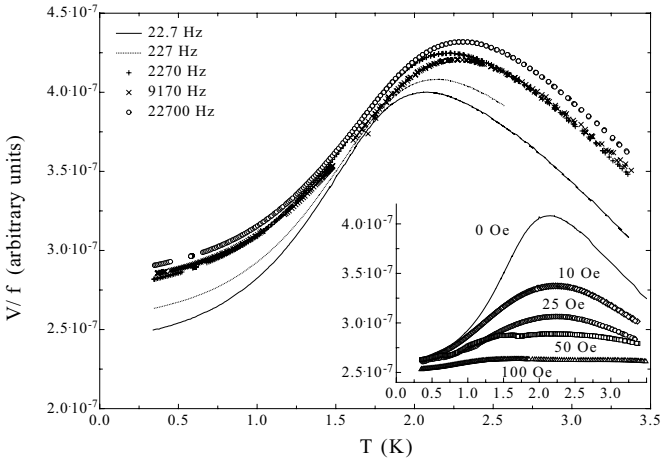

Fig. 3. The response voltage divided by the excitation frequency V/f for $x = 0.77$ as a function of temperature for $f =$ 22.7, 227, 2270, 9170 and 22700 Hz. The inset shows V/f for $f = 227$ Hz in various static magnetic fields.

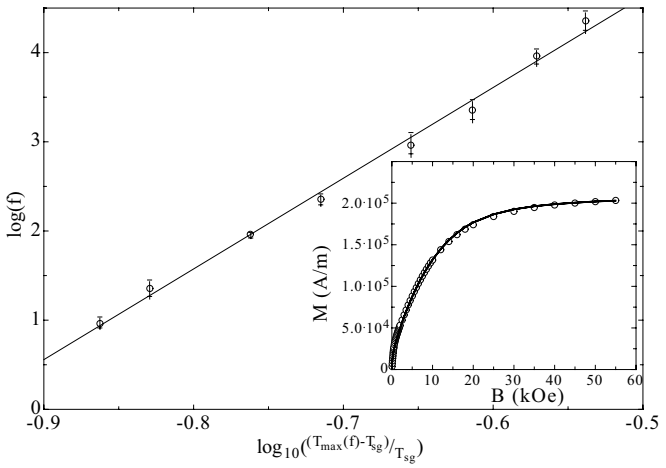

Fig. 4. $log_{10}(f)$ is plotted as a function of $log_{10}[(T_{max}(f) - T_{sg})/T_{sg}]$ for $x = 0.77$. In the inset, we display the measured magnetization $M(H)$ at 2 K for the same sample as empty circles and the calculated curve (solid line) as indicated in the text.

and 3.5 K for $x = 0.73$, 0.77 and 0.84, respectively. The samples were placed into an RCH-1000 plastic cell. Integrated in the cell body were the primary and secondary coil systems, each consisting of a pair of coils with 2×500 and 2×2000 windings, respectively. The current amplitude in the primary coil was of the order of 1 mA and the frequencies of the excitation current were set to $f = 22.7$, 227, 2270, 9170 and 22700 Hz respectively. In Figure 3 we display the output voltage V of the secondary coils, a measure for χ_{ac}, divided by the frequency f, i.e. V/f, versus temperature. The position of the voltage maximum on the temperature scale, $T_{max}(f)$, shifts to higher temperatures upon enhancing the frequency. The application of weak static magnetic fields, of the order of 10 Oe, significantly reduces the amplitude of the maximum. As may be seen in the inset of Figure 3, at and above 100 Oe, the anomaly is completely quenched. This behavior is distinctly different from the features of the ac-susceptibility results for $x = 0.65$ and 0.37, which exhibit a peak at T_C but no observable frequency dependence within experimental resolution.

A frequency dependent maximum in $\chi_{ac}(T)$ is usually taken as evidence for a spin freezing process which leads, upon decreasing the temperature, to a spin-glass configuration, or to the formation of a superparamagnetic phase. Element specific electron microscopy imaging (EFTEM) revealed [4] that material with $x = 0.75$ exhibits an inhomogenous cluster formation with Eu- and Ca rich regions, respectively. This phase separation exceeds the expectations from simply considering the inherent statistical inhomogeneity of the material. The clusters adopt diameters of the order of a few nm. The Eu-rich clusters may be considered as acting like large magnetic molecules with giant magnetic moments. In view of the response of an isolated cluster, its dynamics may be characterized by a relaxation time [15]

$$\tau \equiv 1/f = \tau_0 \cdot e^{E_a/k_B T_B} \quad , \tag{4}$$

where τ_0 is the intrinsic relaxation time of the large moment, E_a represents the energy barrier preventing the reorientation of the moment and T_B denotes the so called blocking temperature. According to literature, however, fitting the available data by employing equation (4) results most often in unrealistic values of these parameters [16]. For real systems, the Vogel-Fulcher relation [17]

$$\tau = \tau_0 \cdot e^{E_a/k_B(T_{max}-T_0)} \quad , \tag{5}$$

describing the frequency dependence of the temperature where the magnetic susceptibility exhibits a maximum, seems to be more appropriate. Here, $k_B T_0$ is the cluster interaction energy. This type of behaviour has often been verified for typical spin glasses [18]. In our case, the best fits are obtained by setting $T_0 = 0$ K, indicating a progressive freezing of moments which interact over a wide range of energies [19]. However, this procedure leads to $\tau_0 \approx 10^{-25}$ s, obviously unrealistic and orders of magnitude different from approximately 10^{-13} s, the common value of τ_0 for conventional spin glasses [20].

In view of the clustering of the Eu moments, a more adequate description of the dynamics is obtained by invoking the critical slowing-down process via

$$f = f_0 \cdot \left(\frac{T_{max}(f) - T_{sg}}{T_{sg}} \right)^{-z\nu} \quad , \tag{6}$$

where T_{sg} is the critical temperature for the spin-glass ordering, $z\nu$ is a constant and $\tau_0 = f_0^{-1}$ is the characteristic time scale for the spin dynamics. In Figure 4 we display our experimental data for $x = 0.77$, together with a fit according to equation (6). The resulting parameters are $T_{sg} = 1.79$ K, $z\nu = 10.17$ and $\tau_0^{-1} = 5.15 \times 10^9$ s^{-1}. For conventional spin glasses, experiments and mean-field calculations yield $z\nu \approx 10$ and $\tau_0 \approx 10^{-12}$ s [16]. It is conceivable that the significant difference in the magnitude of

τ_0 is due to the clustering of ionic moments, forming units with rather large magnetic moments in our case.

It is customary to distinguish between spin-glass and superparamagnetic behaviour on the basis of the value of the ratio [21]

$$K = \frac{\partial \ln(T_{max})}{\partial \ln(f)} \tag{7}$$

where T_{max} is again the temperature at which, for a given frequency f, the maximum of χ_{ac} is observed.

For spin glasses, $K \sim 0.01$ and for superparamagnets, $K \geq 0.1$. For all our samples with $x > 0.7$, we obtain $K \approx 0.06$. Although this does not allow for a clear verdict, we argue that the low-temperature features for these materials are those of a spin glass whereby the freezing does not involve single spin moments, but the total moments of the mentioned Eu-rich clusters.

Additional details of the magnetic response of these ensembles of clusters can be obtained from results of measurements of the field-induced magnetization. In mean field approximation, the magnetization of a single cluster increases with decreasing temperature according to

$$m_{cl} = \mu_{sat} \cdot B_{7/2}\{g\mu_B J(\lambda_{Eu}M + H)/k_B T\} \quad , \tag{8}$$

where $B_{7/2}$ is the Brillouin function for $J = 7/2$, M the sample magnetization, $\lambda_{Eu} = 5.1$ is taken to be identical to the mean field parameter valid for pure EuB_6 [8], H is the external magnetic field and the saturation moment is given by

$$\mu_{sat} = N \cdot \mu_{Eu} \tag{9}$$

i.e., by the number of Eu ions in the cluster and the moment of an individual Eu ion. If the clusters would act independently from each other, the field induced magnetization is expected to vary according to

$$M \sim m_{cl} L\left(\frac{m_{cl}H}{k_B T}\right) \quad , \tag{10}$$

where L represents the Langevin function. It turned out that this approximation is not adequate for describing our $M(H)$ data at low temperatures. The interaction between the clusters can again be taken into account in mean-field approximation, resulting in [22]

$$M(T,H) \sim m_{cl} L\left[\frac{m_{cl}(H + \lambda M(T,H))}{k_B T}\right] \quad , \tag{11}$$

where λ captures the internal field due to the cluster magnetization.

As usual, equation (11) has to be solved self consistently. The corresponding fit to our $M(H)$ data, recorded for the crystal with $x = 0.77$ at $T = 2$ K and displayed in the inset of Figure 4 as open circles, is represented by the solid line. Demagnetization effects for the experimental data have been considered as described in ref. [23]. The average value for $m_{cl} = 260\ \mu_B$ corresponds to a cluster diameter of approximately 3 nm, which is in good agreement with what is observed in the EFTEM images [4]. The molecular-field constant $\lambda = -1.2$ is distinctly smaller than λ_{Eu} and implies that the clusters interact predominantly antiferromagnetically.

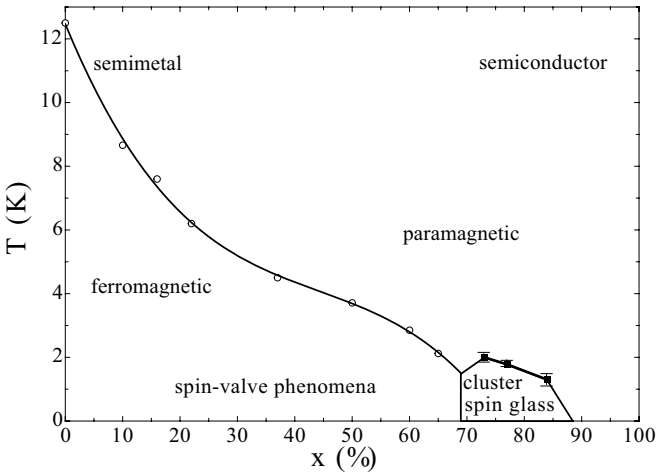

Fig. 5. Phase diagram for $Eu_{1-x}Ca_xB_6$. The open circles denote the ferromagnetic transition obtained from $C_{mag}(T)$ and Arrot-plot analyses [4]. The filled squares represent the cluster spin glass transition temperatures deduced from $\chi_{ac}(T, f)$ data.

3 Conclusion

In summary we provide experimental evidence that for $x > 0.7$ and thus below the site percolation limit, the magnetic ground state of $Eu_{1-x}Ca_xB_6$ is reached via the freezing of moments of sizable Eu-rich clusters. This allows for a completion of the $[x, T]$ phase diagram of this hexaboride series, shown in Figure 5. By increasing x, the material's electronic ground state changes from semimetallic to a semiconducting, where the electronic properties are governed by defect states [24]. We showed previously that, at intermediate concentrations, the inhomogeneous distribution of Eu ions leads to an intrinsic spin-valve features observed in transport and optical properties [14,25]. This experimentally determined phase diagram is in conflict with the conclusions of a recent theoretical calculation based on a simple Kondo lattice model [26]. It appears that the spontaneous formation of Eu-rich clusters, carrying substantial moments, is requested to be a major ingredient in related future theoretical work.

This work has benefited from partial financial support of the Schweizerische Nationalfonds zur Förderung der wissenschaftlichen Forschung and the US-NSF grant DMR-0203214.

References

1. S. Kirkpatrick, Solid State Comm. **12**, 1279 (1973)
2. B.I. Shklovskii, A.L. Efros, Sov. Phys.-Usp. **18**, 845 (1975)
3. W. Henggeler, H.R. Ott, D.P. Young, Z. Fisk, Solid State Commun. **108**, (1998) 929.
4. G.A. Wigger, C. Beeli, E. Felder, H.R. Ott, A.D. Bianchi, Z. Fisk, Phys. Rev. Lett. **93**, 147203 (2004)
5. L. Degiorgi, E. Felder, H.R. Ott, J.L. Sarrao, Z. Fisk, Phys. Rev. Lett. **79**, 5134 (1997)

6. D. Mandrus, B. C. Sales and R. Jin, Phys. Rev. B **64**, 12302 (2001)
7. C. Kittel, *Introduction to Solid State Physics* (J. Wiley and Sons, New York 1967)
8. G.A. Wigger, R. Monnier, H.R. Ott, D.P. Young, Z. Fisk, Phys. Rev B **69**, 125118 (2004)
9. S. Süllow, I. Prasad, M.C. Aronson, S. Bogdanovich, J.L. Sarrao, and Z. Fisk, Phys. Rev. B **62**, 11626 (2000)
10. J.C. Cooley, M.C. Aronson, J.L. Sarrao, Z. Fisk, Phys. Rev. B **56**, 14541 (1997)
11. S. Süllow, I. Prasad, M.C. Aronson, J.L. Sarrao, Z. Fisk, D. Hristova, A.H. Lacerda, M.F. Hundley, A. Vigliante, D. Gibbs, PRB **57**, 5860 (1998)
12. M C. Aronson, J.L. Sarrao, Z. Fisk, M. Whitton, B.L. Brandt, Phys. Rev. B **59**, 4720 (1999)
13. S. Paschen, D. Pushin, M. Schlatter, P. Vonlanthen, H.R. Ott, D.P. Young, Z. Fisk, Phys. Rev. B **61**, 4174 (2000)
14. G.A. Wigger, C. Wälti, H.R. Ott, A.D. Bianchi, Z. Fisk, Phys. Rev. B **66**, 212410 (2002)
15. L. Néel, Ann. Geophys. **5**, 99 (1949)
16. J.A. Mydosh, *Spin-Glasses: An Experimental Introduction* (Taylor and Francis, London, 1993)
17. S. Shtrikman, E.P. Wohlfarth, Phys. Lett. A **85**, 467 (1981)
18. F. Holtzberg, T.L. Francavilla, C.Y. Huang, J.L. Tholence, J. Appl. Phys. **53**, 2229 (1982)
19. H.v. Löhneysen, J.L. Tholence, J. Magn. Magn. Materials **13**, 136 (1979)
20. K. Gunnarson, P. Svedlindh, P. Nordblad, L. Lundgren, H. Aruga, A. Ito, Phys. Rev. Lett. **61**, 754 (1988)
21. G.V. Bazuev, O.V. Makaroa, G.P. Sheveikin, Russ. J. Inorg. Chem. **28**, 1088 (1983)
22. L. Wang, J. Ding, Y. Li, H.Z. Kong, Y.P. Feng, X.Z. Wang, J. Phys: Condens. Matter **12**, 4253 (2000); or L. Wang, J. Ding, Y. Li, Y.P. Feng, N.X. Phuc, N.H. Dan, J. App. Phys. **89**, 8046 (2001)
23. C. Kittel, *Introduction to Solid State Physics* (John Wiley and Sons, New York 1967)
24. K. Giannó, A.V. Sologubenko, H.R. Ott, A.D. Bianchi, Z. Fisk, J. Phys: Cond Matter **14**, (2002) 1035
25. A. Perucchi, G. Caimi, H.R. Ott, L. Degiorgi, A.D. Bianchi, Z. Fisk, Phys. Rev. Lett **92**, 067401 (2004)
26. V.M. Pereira, J.M.B. Lopes dos Santos, E.V. Castro, A.H. Castro Neto, Phys. Rev. Lett. **93**, 147202 (2004)